

**CRYSTALLIZATION STUDY ON SYNTHETIC FLUORINE FREE SLAGS**

E. Brandaleze\*, E. Benavidez, L. Santini

Departamento de Metalurgia, Facultad Regional San Nicolás, Universidad Tecnológica Nacional, Colón 332, San Nicolás, (2900), Argentina.

\*Corresponding author: [ebbrandaleze@frsn.utn.edu.ar](mailto:ebbrandaleze@frsn.utn.edu.ar), phone: 54-336-4420830 ext. 217, 54-336-4420820

Recibido: Abril 2012 Aprobado: Octubre 2012

Publicado: Enero 2013

**ABSTRACT**

The horizontal heat extraction and lubrication are considered key factors in the continuous casting of the steel in order to avoid product defects and operation problems. Synthetic slags named mould fluxes are used to achieve good lubrication and controlled heat transfer. Commercial mould fluxes are constituted by several oxides, fluorine compounds and carbonaceous materials. The fluorine compounds control physical properties and have relevant influence on the crystallization of the slag during casting operation. Nevertheless, fluorine emissions during operation could cause health problems and equipment corrosion. For these reasons, nowadays fluorine free mould fluxes are developed.

In order to compare the crystallization process of mould fluxes (with and without fluorine compounds) samples of both types of fluxes were melted, quenched and heat treated at 600°C, 700°C and 850 °C. Samples were identified as: A (with 10.4 % of F), B (with 6% B<sub>2</sub>O<sub>3</sub>) and BL (with 6% B<sub>2</sub>O<sub>3</sub>, 4% Li<sub>2</sub>O). It is relevant to mention that the proportion and type of crystalline phases affect the thermal conductivity of the mould fluxes during steel solidification. Also, the viscosity behaviour is affected by crystallization process. In this paper, a microscopy study was carried out applying light and scanning electron microscopy (SEM) on all the samples. The information was correlated with DTA and X ray diffraction (XRD) results obtained at different temperatures. The chemical composition of phases was determined by EDS (SEM). The information obtained allows us to identify the crystallization mechanism in all the samples and increase the knowledge on fluorine free mould flux behaviour in the continuous casting mould. In the specimens BL it was detected a liquid-liquid phase separation process prior to crystallization.

**Keywords:** crystallization, microscopy, mold fluxes, continuous casting, steel.

**ESTUDIO DE CRISTALIZACIÓN DE ESCORIAS SINTÉTICAS LIBRES DE FLÚOR****RESUMEN**

La extracción térmica horizontal y la lubricación representan factores clave para evitar la generación de defectos en productos o de problemas operativos en la colada continua de aceros. Las escorias sintéticas, denominadas polvos coladores, brindan una buena lubricación y suministran una extracción térmica controlada. Estos polvos coladores están constituidos por una mezcla de óxidos, compuestos con flúor y materiales carbonosos. Los compuestos con flúor inciden en las propiedades físicas y en la cristalización de los polvos durante la operación de colada. En la actualidad, preocupa la emisión de gases que pueden generarse durante el proceso dado que pueden ocasionar problemas de salud en los operarios y daños sobre los equipos industriales. Por esta razón, se hallan en desarrollo polvos coladores libres de flúor.

Con el objetivo de comparar el proceso de cristalización que se desarrolla en polvos sin y con flúor, se fundieron, enfriaron y luego trataron térmicamente a temperaturas de 600°C, 700°C y 850 °C muestras con diferentes composiciones: A (con 10.4 % F), B (con 6% B<sub>2</sub>O<sub>3</sub>) y BL (con 6% B<sub>2</sub>O<sub>3</sub> y 4% Li<sub>2</sub>O). Resulta relevante mencionar que la proporción y tipo de fases cristalinas presentes, afecta la conductividad térmica del polvo colador durante la solidificación del acero. También, el comportamiento de la viscosidad es afectado por la cristalización del polvo colador. En este trabajo, se presentan resultados de un estudio de microscopía óptica y electrónica de barrido (SEM) realizado sobre todas las muestras. La información obtenida se correlaciona con resultados de DTA y difracción de rayos X (DRX) realizados a diferentes temperaturas. Esta información ha permitido identificar los mecanismos de cristalización en todas las muestras y predecir el comportamiento de los polvos libres de flúor en el molde de la colada continua.

**Palabras clave:** cristalización, microscopía, polvos coladores, colada continua, aceros.

**INTRODUCTION**

Mould fluxes play an important role in the continuous casting of steel. Important functions such as: prevention

of liquid steel oxidation, providing lubrication at mould/metal interface, control of the heat transfer and improving inclusion absorption. These mould fluxes

usually contain (4 to 10 %) of  $\text{CaF}_2$ . The purpose of fluoride addition is to decrease slag viscosity, break temperature (to improve lubrication) and to control heat transfer through the precipitation of cuspidine ( $3\text{CaO}\cdot 2\text{SiO}_2\cdot \text{CaF}_2$ ) at the mould-strand gap [1-3].

At casting conditions, fluorides promote gaseous species emissions such as:  $\text{SiF}_4$  produced by  $\text{CaF}_2$  and  $\text{SiO}_2$  reaction in the slag, HF formation by reactions between water stream and gaseous compounds. Both  $\text{SiF}_4$  and HF contribute to acid rain, pollution of ground water from wasted slags and they pose a potential health and safety hazard [4].

The gaseous emissions also alter the slag chemistry, thus influencing their physical properties and crystallization process.

Fox et al. in [5] present a study on  $\text{B}_2\text{O}_3$  and  $\text{Na}_2\text{O}$  as alternative substitutes for  $\text{CaF}_2$  in billet fluxes. They also report that the new flux has been successfully tested in an industrial plant. The authors considered the influence of both oxides on the viscosity and break temperature. Fox also report results on crystallization of fluxes that contain 1.5 % and 4 %  $\text{B}_2\text{O}_3$ .

In previous papers, we also informed the influence of  $\text{B}_2\text{O}_3$  and  $\text{Li}_2\text{O}$  on the viscosity, melting temperature and fluidity behavior. For (6%) of  $\text{B}_2\text{O}_3$  addition in the slag critical temperatures were adjusted to the required values, but the fluidity degree was not high enough. When the addition consisted in  $\text{B}_2\text{O}_3$  (6%) and  $\text{Li}_2\text{O}$  (4%) a similar fluidity (respect the mould flux with  $\text{CaF}_2$ ) was obtained. Nevertheless, the critical temperatures: softening point, hemisphere point and fluidity point, present a considerable decrease [6].

The aim of this paper is to increase the knowledge on the crystallization mechanism and behavior of the fluxes with different content of  $\text{B}_2\text{O}_3$  and  $\text{Li}_2\text{O}$  with respect to the fluxes that contain  $\text{CaF}_2$  in order to predict the heat transfer in the mould.

## MATERIALS AND METHODS

The chemical composition of the mould fluxes selected for this study and their basicity index (BI) is presented

in table 1. In this table, “others” include:  $\text{K}_2\text{O}$  (0.7%),  $\text{Fe}_2\text{O}_3$  (1.6%),  $\text{TiO}_2$  (0.2%),  $\text{P}_2\text{O}_5$  (0.7%).

### Sample preparation.

Samples of 15 g were melted in a platinum crucible at  $1300^\circ\text{C}$ . Then they were poured, quenched and heat treated at:  $600^\circ\text{C}$ ,  $700^\circ\text{C}$ ,  $850^\circ\text{C}$ , in order to characterize the crystallization mechanism.

Different times in heat treatments were considered: 15, 60 and 180 min.

All samples were molded in a polyester resin, polished by water proof paper, diamond paste and finally alumina slurry. Then, they were etched with nital 2 % for a few seconds.

**Table 1.** Chemical composition and basicity index (BI) of the mould fluxes.

Sample	A	B	BL
$\text{SiO}_2$	36.2	35.7	34.3
$\text{CaO}$	30.8	31.3	30.1
$\text{MgO}$	2.1	2.1	2.0
$\text{Al}_2\text{O}_3$	5.1	5.2	4.7
$\text{Na}_2\text{O}$	12.7	20.0	19.0
F	10.4	-	-
$\text{B}_2\text{O}_3$	-	5.9	5.9
$\text{Li}_2\text{O}$	-	-	3.9
Others	3.2	-	-
<b>BI</b>	0.85	0.88	0.88

The microstructure of the samples was observed by light microscopy using an Olympus GX51 microscope, with a Leco IA 32 image analysis system. The thickness of the surface columnar crystal layer was measured (on cross sections) applying the linear technique and particle quantification was carried out on 7 fields (area of  $0,630\text{ mm}^2$ ) at (500x). The study was completed with scanning electron microscopy SEM using a FEI Quanta 2000. The crystal phase evolution at different temperatures was established by X ray diffraction applying Philips X'Pert. Crystalline phases were identified by Match software (Crystal Impact) version

1.11. The thermal behaviour of the mould fluxes was determined by DTA (Shimadzu DTG60-H).

## RESULTS AND DISCUSSION

### Structural aspect of the samples.

**Sample A** (with 10.4%CaF<sub>2</sub>) quenched and heat treated at different temperatures: 600, 700 and 850°C, were observed by light microscopy.

In the case of sample A-600 °C-60 min, the structure at the surface presents a columnar crystal layer of 40 µm of thickness. Inside the sample, numerous (irregular) white crystals are identified. This affirmation is in accordance with the information reported in a previous paper [7], figure 1.

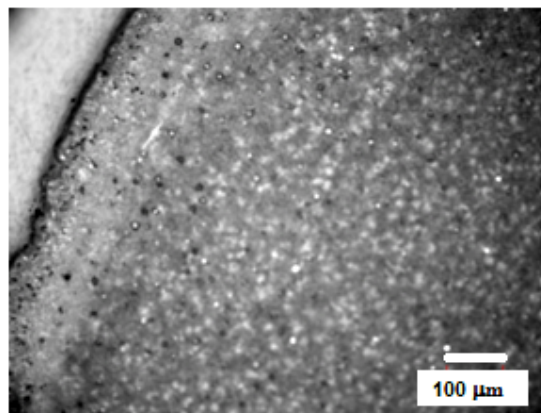


**Fig. 1.** Structural aspect of the sample A-600 °C-60 min.

The X ray diffraction results obtained on this sample at different conditions (as quenched and treated at 600 to 850°C) is observed in figure 2. The as quenched sample shows a glassy behaviour, but from 600 °C to 850°C crystalline peaks are observed. The main crystal phase (around  $\theta \approx 30^\circ$ ) corresponds to cuspidine ( $3\text{CaO}\cdot 2\text{SiO}_2\cdot \text{CaF}_2$ ) and it is present at all temperatures. At 850°C nepheline ( $\text{Al}_4\text{Ca}_{0.4}\text{K}_{0.8}\text{Na}_2\text{Si}_4$ ) and villiaumite (NaF), were also identified.

DTA results corroborate the crystallization of the phases in the sample A with peaks: (P<sub>1</sub>) of cuspidine ( $3\text{CaO}\cdot 2\text{SiO}_2\cdot \text{CaF}_2$ ) at 610°C, (P<sub>2</sub>) nepheline

( $\text{Al}_4\text{Ca}_{0.4}\text{K}_{0.8}\text{Na}_2\text{Si}_4$ ) at 729 °C and villiaumite (NaF) at 854 °C (Figure 3).

The crystal phases of sample A were observed by SEM and analyzed by Energy Dispersive X-Ray Spectroscopy (EDS) in order to corroborate the presence of cuspidine ( $3\text{CaO}\cdot 2\text{SiO}_2\cdot \text{CaF}_2$ ), nepheline ( $\text{Al}_4\text{Ca}_{0.4}\text{K}_{0.8}\text{Na}_2\text{Si}_4$ ) and villiaumite (NaF). Figure 4, shows the villiaumite (NaF) precipitated in the cuspidine ( $3\text{CaO}\cdot 2\text{SiO}_2\cdot \text{CaF}_2$ ) matrix.

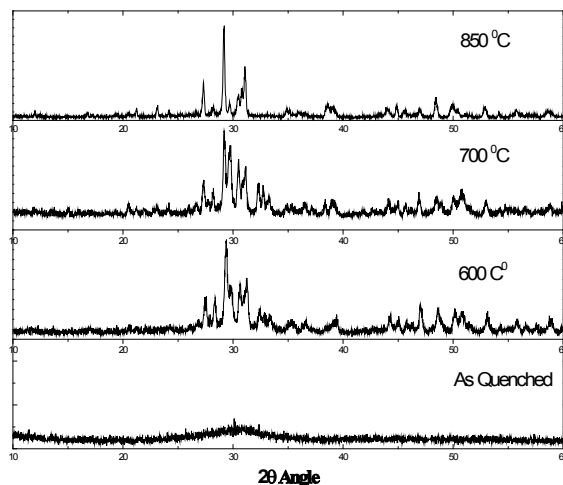


**Fig 2.** X ray diffraction results obtained on sample A.

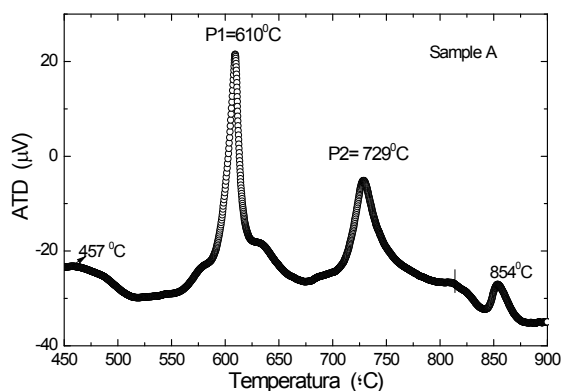


**Fig 3.** DTA results of sample A during heating.

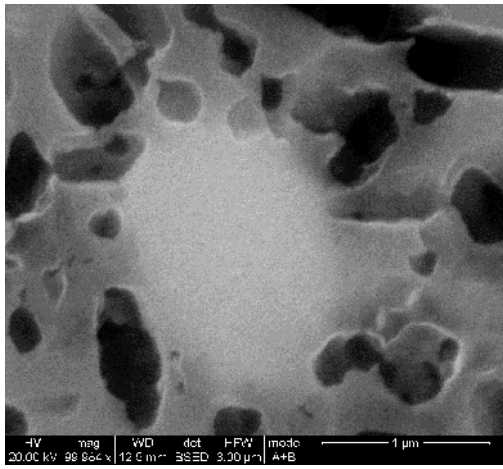


**Fig 4.** Villiumite (NaF) phase precipitated in a cuspidine (3CaO.2SiO<sub>2</sub>.CaF<sub>2</sub>) matrix.

The crystallization mechanism observed in sample A at higher temperatures (700°C and 850°C) is in complete agreement with the mechanisms informed in [7].

Sample B (with 6% B<sub>2</sub>O<sub>3</sub>), treated at 600°C - 60 min present a columnar crystal layer at the surface (similarly to sample A) and the thickness is 150 μm. Nevertheless, inside the sample the structure indicates the presence of a liquid immiscibility phenomena (figure 5).

Rincón and Durán [8], described this phenomena associated with two amorphous (glassy) phases separation. It is produced in systems that are rich in SiO<sub>2</sub> in combination with alkaline oxides (RO-SiO<sub>2</sub>) like the studied slags. During slag quenching, below T<sub>g</sub> = 454°C temperature (figure 10) micro droplets of a glassy phase are separated respect to another glassy phase. The mentioned authors studied extensively the liquid immiscibility on different systems, including Na<sub>2</sub>O-B<sub>2</sub>O<sub>3</sub>-SiO<sub>2</sub>, similar to sample B. It is possible to consider the presence of a metastable liquid immiscibility (or a subliquidus). The heat treatment at 600°C (between the transformation temperature and the immiscibility curve) promoted spherical nuclei formation, figure 5. The nuclei were quantified by light microscopy and the average number is: 1053 nuclei/area (0,630 mm<sup>2</sup>).

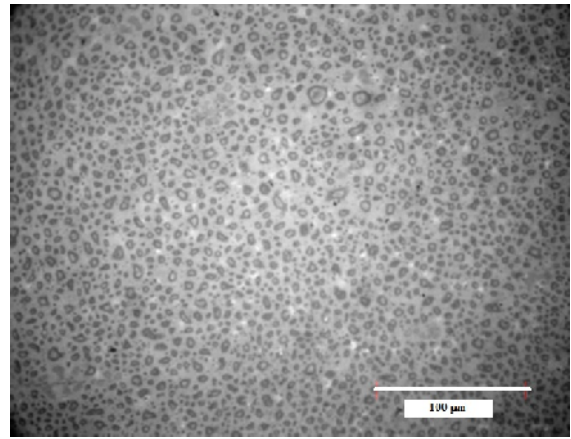


**Fig 5.** Spherical nuclei present in the structure of sample B-600 °C-60 min (with B<sub>2</sub>O<sub>3</sub> 6%).

**Sample BL** (6%B<sub>2</sub>O<sub>3</sub> and 4%Li<sub>2</sub>O), treated at 600 °C - 60 min, (below T<sub>g</sub> = 548°C, figure 10) also presents a columnar crystal layer in the surface and its thickness is 130 μm. Inside the sample the structure also presents spherical nuclei showing a metastable liquid immiscibility appearance (Figure 6).

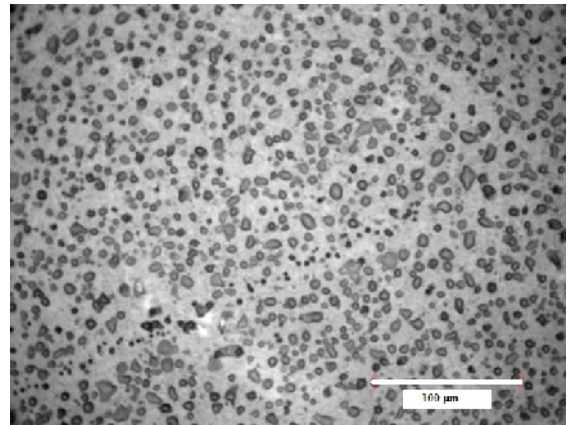


**Fig 6.** Immiscible liquid appearance observed in sample BL-600 °C-60 min (6% B<sub>2</sub>O<sub>3</sub> and 4% Li<sub>2</sub>O).

The average number of nuclei in this sample was 756 nuclei / area. It is relevant to comment that in localized zones of the sample BL, clusters of nuclei were identified (Figure 7).

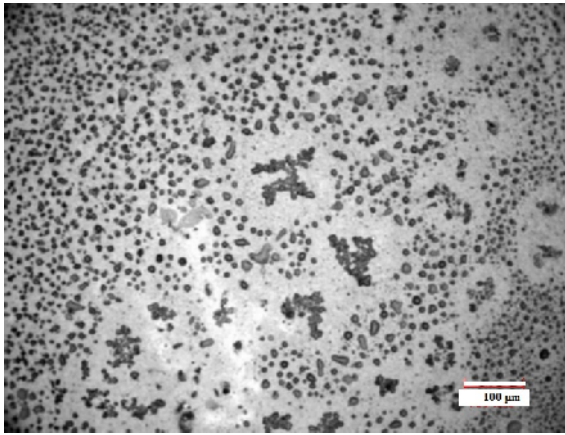


**Fig 7.** Clustering of spherical particles observed in sample BL-600 °C-60 min (6% B<sub>2</sub>O<sub>3</sub> and 4% Li<sub>2</sub>O).

Rincón and Durán [8] mentioned that when nuclei are formed, the droplets growing occur through a controlled diffusion process and also the liquid separation precedes the crystallization process. By this mechanism the crystallization is more homogeneous. In agreement with this affirmation it is possible to think that a lower number of nuclei per area associated with the presence of nuclei clusters indicate that the crystallization process is close to the initial stage.

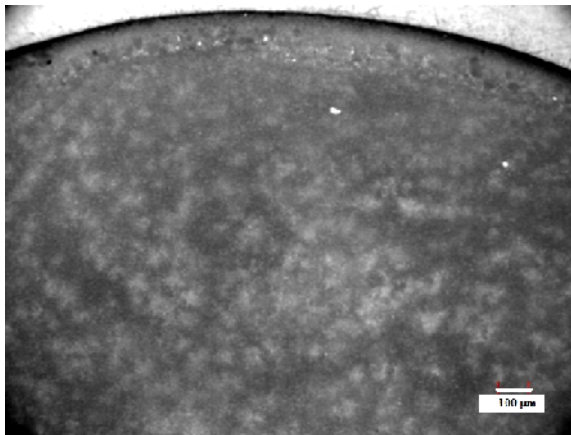


**Fig 8.** Structure aspect of the sample BL-850 °C-60 min (6% B<sub>2</sub>O<sub>3</sub> and 4% Li<sub>2</sub>O).

At higher temperatures ( $\approx 850^\circ\text{C}$  in B and  $\approx 900^\circ\text{C}$  in BL) the spherical nuclei disappear and crystalline phases are visualized in both samples. Figure 8 shows the structure of sample BL (heat treated at  $850^\circ\text{C}$ ) with white crystal phases in the bulk of the specimen. The

structure is quite similar respect to sample A-600 °C-60 min.

In samples B and BL, X ray diffractograms show presence of a primary combeite (Na<sub>2</sub>Ca<sub>2</sub>Si<sub>3</sub>O<sub>9</sub>) crystalline phase, peak around  $\theta \approx 35^\circ$ , at temperatures  $650^\circ\text{C}$  (B) and  $710^\circ\text{C}$  (BL) (figure 9).

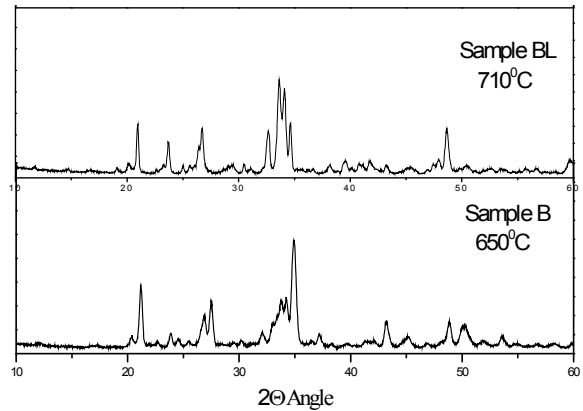


**Fig 9.** X Ray diffractograms obtained on samples B and BL.

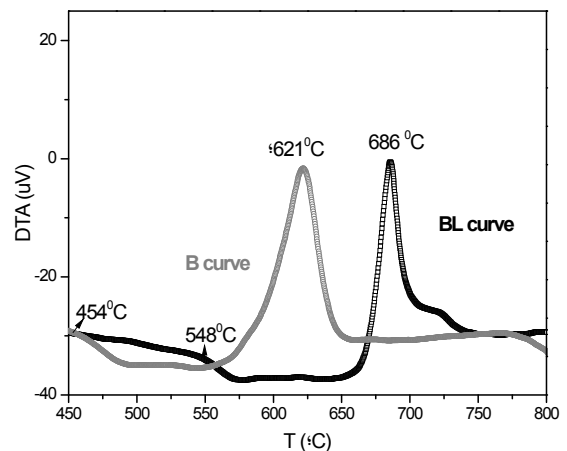


**Fig 10.** DTA results of the samples B and BL during heating.

In B and BL samples, the crystallization mechanisms show also a glassy structure in the as quenched samples. At  $600^\circ\text{C}$  both samples (B and BL) present a columnar crystal layer of combeite (Na<sub>2</sub>Ca<sub>2</sub>Si<sub>3</sub>O<sub>9</sub>) in the surface. These result agree with the XRD results that present the main peak at  $\theta \approx 35^\circ$ . The similar thickness and crystalline phase of the columnar crystal surface layer in both cases B-150  $\mu\text{m}$  and BL-130  $\mu\text{m}$  suggest a similar kinetic of crystallization. However, a minimum



thickness of 40  $\mu\text{m}$  in the columnar crystal layer was determined in sample A. The crystallization process is controlled by supercooling and it is possible to adjust this variable in order to achieve similar crystallization rates. The liquid immiscibility phenomenon presented in B and BL samples allows us to predict a more homogeneous crystallization process of the slags at process conditions. The differences of nuclei densities in the samples: 1053 nuclei/area (sample B) and 756 nuclei/area (sample BL) are justified because of different viscosity values between samples at the melting condition [7]: B ( $\eta_{1300^\circ\text{C}} = 2.18 \text{ dPa}\cdot\text{s}$ ) and BL ( $\eta_{1300^\circ\text{C}} = 1.10 \text{ dPa}\cdot\text{s}$ ). At 621 $^\circ\text{C}$  for sample B and 686 $^\circ\text{C}$  for sample BL, the combeite ( $\text{Na}_2\text{Ca}_2\text{Si}_3\text{O}_9$ ) crystallization starts inside the sample.

Based on the DTA results it is possible to confirm that sample B (with 6%  $\text{B}_2\text{O}_3$ ) crystallizes at 621 $^\circ\text{C}$ , closer to sample A than BL (6% $\text{B}_2\text{O}_3$  and 4% $\text{Li}_2\text{O}$ ), that crystallizes at 686 $^\circ\text{C}$ .

B and BL surface columnar crystal layer of combeite ( $\text{Na}_2\text{Ca}_2\text{Si}_3\text{O}_9$ ) are thicker (150  $\mu\text{m}$ , 130  $\mu\text{m}$  respectively) than the cuspidine layer (3  $\text{CaO}\cdot 2\text{SiO}_2\cdot \text{CaF}_2$ ) of sample A (40  $\mu\text{m}$ ).

Zuo et al. in [4] and Kim et al in [9] confirm that the evaporation of  $\text{Na}_2\text{O}$ ,  $\text{B}_2\text{O}_3$  and  $\text{Li}_2\text{O}$  are negligible at similar conditions respect to operation melting period in the continuous casting of steel. This affirmation allows us to consider the slags (B and BL) as possible mould fluxes because they exhibit good crystallization kinetic and physical properties, similar to those of sample A. Therefore,  $\text{B}_2\text{O}_3$  and  $\text{Li}_2\text{O}$  oxides represent an alternative replacement for fluorine ( $\text{CaF}_2$ ).

## CONCLUSIONS

The microscopy study applying light and scanning electron microscopy (SEM) with EDS provide key information to identify the crystallization mechanisms developed in all samples: A (10.4 % F), B (6%  $\text{B}_2\text{O}_3$ ) and BL (6%  $\text{B}_2\text{O}_3$ , 4%  $\text{Li}_2\text{O}$ ).

In samples B (6%  $\text{B}_2\text{O}_3$ ) and BL (6%  $\text{B}_2\text{O}_3$ , 4%  $\text{Li}_2\text{O}$ ), a phenomena of liquid immiscibility was identified previous to the crystallization process of the mould powder. This phenomenon in sample A (10.4 % F) at the same temperature (600 $^\circ\text{C}$ ), was not observed. It is important to remark the importance of the microscopy techniques to visualize these phenomena that have an important influence on mould fluxes properties and crystallization process at process conditions.

The correlation between XRD, DTA and microscopy results obtained by EDS (SEM), allow us to identify the crystalline phases in each sample.

Similar crystallization temperatures suggest the possibility of the  $\text{CaF}_2$  substitution by  $\text{B}_2\text{O}_3$  and  $\text{Li}_2\text{O}$  oxides.

## REFERENCES

- [1] Persson M., Seetharaman S. and Seetharaman S., (2007) "Kinetic studies of fluoride evaporation from slags", *ISIJ International*, 47: 12, pp.1711-1717.
- [2] Susa M., Kushimoto A. and Kobayashi Y., (2011) "Controllability of radiative heat flux across mould flux films by cuspidine grain size", *ISIJ International*, 51: 10, pp.1587-1596.
- [3] Hooli P., (2003), "Mould flux film between mould and steel Shell – Effect of heat flux and defect formation", *Steel Research*, 74, 8, pp. 480-484.
- [4] Zuo Tai Z., Seetharaman S., Jung W. C., (2011) "An investigation of the evaporation of  $\text{B}_2\text{O}_3$  and  $\text{Na}_2\text{O}$  in F- free mold slags", *ISIJ International*, 51: 1, pp. 80-87.
- [5] Fox A. B., Mills K. C., Lever D., Bezerra C. Valadares C. and Unamuno I., (2005) "Development of fluoride – free fluxes for billet casting", *ISIJ International*, 45: 7, pp.1051-1058.
- [6] Benavidez E., Martin A., Brandaleze E., Valentini M., Santini L., Rodriguez D. and González Oliver C., (2009), "Melting and fluidity behaviour on mold fluxes with fluorine-free alternative compositions", *17<sup>th</sup> IAS Steelmaking Conference 2009*, pp. 251-258.

- [7] Santini L., Benavidez E. and Brandaleze E., (2010), “Evaluation of the mold fluxes crystallization by microscopy techniques”, *Acta Microscopica*, 19, 1, pp. 1 – 8.
- [8] Rincón J.M. and Durán A., (1982), “*Separación de fases en vidrios – El sistema  $Na_2O-B_2O_3-SiO_2$* ”, Madrid, Sociedad Española de Cerámica y Vidrio, Arganda del Rey, pp. 15-96.
- [9] Kim G. H. and Sohn I., (2012) “Influence on the viscous behavior of CaO- $Al_2O_3$ -12 mass %  $Na_2O$ -12 mass %  $CaF_2$  based slags”, *ISIJ International*, 52: 1, pp. 68-73.